New Journal of Physics
The open-access journal for physics

Anisotropic susceptibility of $La_{2-x}Sr_xCoO_4$ related to the spin states of cobalt

N Hollmann[1,3], M W Haverkort[1], M Cwik[1], M Benomar[1], M Reuther[1], A Tanaka[2] and T Lorenz[1]

[1] II Physikalisches Institut, University of Cologne, Zülpicherstrasse 77, D-50937 Köln, Germany
[2] Department of Quantum Matter, ADSM, Hiroshima University, Higashi-Hiroshima 739-8530, Japan
E-mail: hollmann@ph2.uni-koeln.de

New Journal of Physics **10** (2008) 023018 (9pp)
Received 12 November 2007
Published 13 February 2008
Online at http://www.njp.org/
doi:10.1088/1367-2630/10/2/023018

Abstract. We present a study of the magnetic susceptibility of $La_{2-x}Sr_xCoO_4$ single crystals in a doping range $0.3 \leqslant x \leqslant 0.8$. Our data show a pronounced magnetic anisotropy for all compounds. This anisotropy is in agreement with a low-spin ground state ($S = 0$) of Co^{3+} for $x \geqslant 0.4$ and a high-spin ground state ($S = 3/2$) of Co^{2+}. We compare our data with a crystal-field model calculation assuming local moments and find a good description of the magnetic behavior for $x \geqslant 0.5$. This includes the pronounced kinks observed in the inverse magnetic susceptibility, which result from the anisotropy and low-energy excited states of Co^{2+} and are not related to magnetic ordering or temperature-dependent spin-state transitions.

[3] Author to whom any correspondence should be addressed.

Transition-metal oxides are known for their complex interplay between different degrees of freedom like spin, charge and orbitals. In some of these systems another interesting property is found: ions like Co^{3+} in a crystal-field environment can occur in different spin states. Additionally, transitions between different spin states are possible for some compounds. A prominent example showing this phenomenon is $LaCoO_3$, which has been examined and discussed since the middle of the last century (see e.g. [1]–[11]).

The existence of different spin states arises from the competition between crystal-field effects and on-site Coulomb interaction. Crystal fields lift the degeneracy of the 3d states. If the crystal field is strong, this can lead to a violation of Hund's rules. In the case of cubic symmetry and in a one-electron picture, the five-fold degenerate 3d states are split into a three-fold degenerate t_{2g} and a two-fold degenerate e_g level. The splitting between t_{2g} and e_g states is called $10Dq$. With a strong crystal field, the electrons will be forced into the low-spin state (LS). Regarding a $3d^6$ system, this state consists of an antiparallel alignment of spins with $t_{2g}^6 e_g^0$ and $S = 0$. On the other hand, the Coulomb interaction manifests itself in the effect of Hund's coupling. A parallel arrangement of spins minimizes the electron–electron repulsion because the Pauli principle forces the electrons to occupy different orbitals. In a weak cubic crystal field, this effect will dominate and lead to the high-spin state (HS), which is the configuration with the highest total spin possible in accordance with the Pauli principle. For a $3d^6$ system, this configuration is $t_{2g}^4 e_g^2$ with $S = 2$. For Co^{3+} the crossover between these two different spin states occurs roughly at an energy difference of $10Dq = 2.2\,\text{eV}$.

In the case of $LaCoO_3$, a low-spin ground state for Co^{3+} was found [2]. Interestingly, the difference between the crystal field energies and the promotional energies is so small that an excited state with different spin state can be reached by thermal excitation. This excited state has been a subject of debate for a long time. Apart from the HS state described above, the intermediate-spin state (IS, $t_{2g}^5 e_g^1$ $S = 1$) was also discussed [4] and reported in many experiments, but it was shown that it might have been confused with a spin–orbit coupled HS state [11].

For the layered cobaltates $La_{2-x}Sr_xCoO_4$, much less is known about the spin state of Co^{3+}. Based on magnetic measurements [12] a HS ground state for $x \leqslant 0.7$ and a spin-state transition to an IS ground state for $x > 0.7$ were proposed. This conclusion was based on a Curie–Weiss analysis of the susceptibility in a temperature range of 100–300 K and NMR measurements [13]. Unrestricted Hartree–Fock calculations [14] showed a slightly different picture. Here, three different magnetic phases were found. An antiferromagnetic HS phase ($x < 0.39$), a ferromagnetic HS phase ($0.39 \leqslant x \leqslant 0.52$) and an antiferromagnetic LS–HS-ordered phase ($x > 0.52$) were proposed. These calculations were also based on the results of the Curie–Weiss analysis in [12]. Taking into account that $La_{2-x}Sr_xCoO_4$ is an anisotropic material with rather strong spin–orbit coupling compared to the tetragonal crystal field splitting, the validity of the Curie–Weiss law is questionable. The aim of this paper is to analyze the magnetic susceptibility from a different perspective, concentrating on the spin state of Co^{3+}.

The single crystals used for the magnetic measurements have been grown using the floating-zone technique in an image furnace. A strontium doping range of $0.3 \leqslant x \leqslant 0.8$ was covered. Resistivity measurements revealed that $La_{2-x}Sr_xCoO_4$ is a strong insulator for all Sr doping concentrations. The $x = 0.5$ sample turned out to possess the highest resistivity, which is in accordance with the charge ordering of Co^{2+} and Co^{3+} at $\approx$750 K that has already been reported [15].

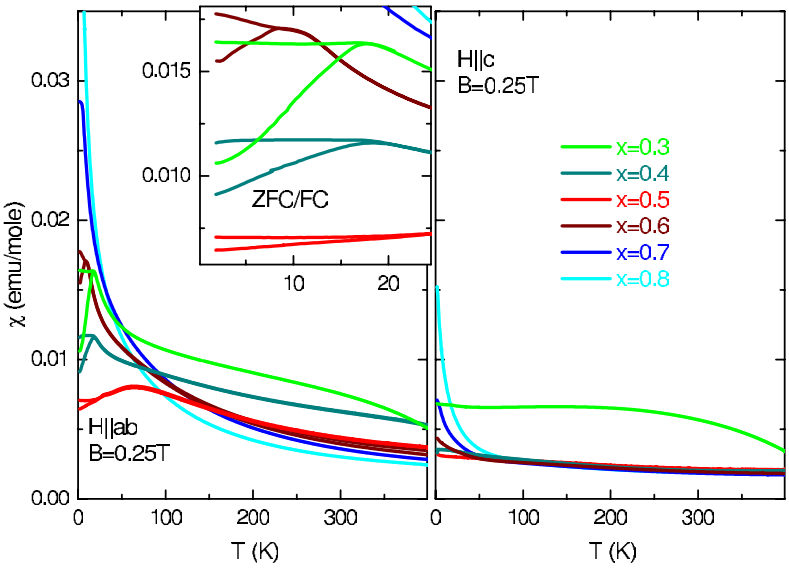

Figure 1. Magnetic susceptibility of $La_{2-x}Sr_xCoO_4$ for two different directions of the magnetic field. The insert is an expanded view of the low-temperature region to show the difference between field cooled (FC) and zero-field cooled (ZFC) measurements for $0.3 \leqslant x \leqslant 0.6$. The curves with the lower susceptibility refer to the ZFC measurements.

The magnetization was measured with a Quantum Design vibrating sample magnetometer (VSM). The field was aligned parallel to the CoO_2 planes as well as perpendicular to these planes (the crystallographic *c*-direction). The corresponding components χ_{ab} and χ_c are plotted in figure 1. A short-range antiferromagnetic order has been found in the compounds $0.3 \leqslant x \leqslant 0.6$ by neutron measurements [16]. This frustrated short-range order is also reflected by the difference between FC and ZFC measurements at low temperatures. The susceptibility is smaller for ZFC than FC below a certain freezing temperature.

Figure 2 shows the inverse magnetic susceptibility for both orientations of field. The main feature of the susceptibility in the paramagnetic regime is the pronounced magnetic anisotropy, both in magnitude and form of the curves. The direction of the anisotropy is the same for all crystals, finding χ_{ab} to be bigger than χ_c.

Here, the magnetic anisotropy arises from band structure and spin–orbit coupling. For Mott and charge-transfer insulators with well-localized moments, band-structure and covalency effects can be approximated by an effective crystal field. The crystal field reflects the anisotropy of the lattice and lifts the degeneracy of the 3d states, resulting in a new set of linear combinations of the unperturbed wavefunctions as a basis. The expectation values of the components of the orbital moment result from these new linear combinations. Thus, the crystal's anisotropy may result in an anisotropy of the orbital moment. Spin–orbit coupling ties the spin moment to this anisotropy. The spin–orbit coupling Hamiltonian will be written as $\zeta \sum_i l_i \cdot s_i$ where the sum over i runs over all electrons. The dot product between spin and orbital momentum tends to align these moments antiparallel for each electron. For an anisotropic orbital momentum, the spin is aligned in the direction of maximum orbital momentum [17].

The full many-body ground-state for a d^6 or d^7 configuration in a crystal-field calculation including spin–orbit coupling and tetragonal distortions is not simple [18] but well known.

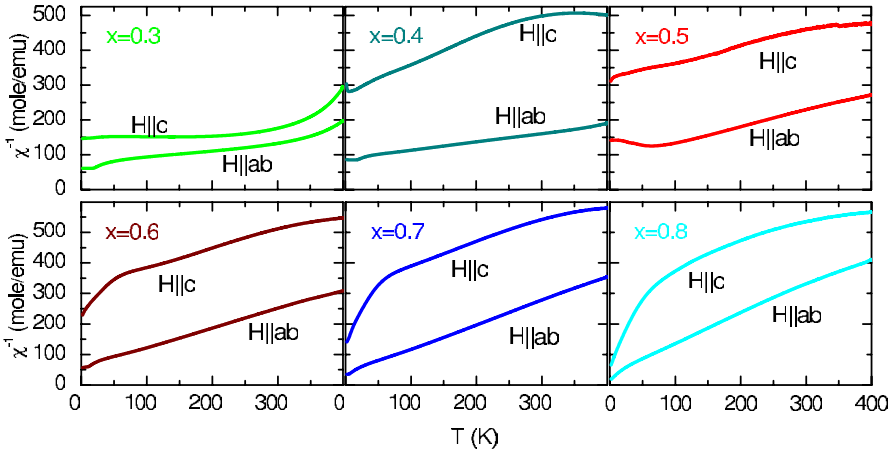

Figure 2. Inverse susceptibility of $La_{2-x}Sr_xCoO_4$ for two different directions of the magnetic field. The form of the curves and the magnetic anisotropy strongly deviate from Curie–Weiss behavior.

In order to get an intuitive picture one would like to fall back on a single electron description. In the limit of full spin polarization this can be done and gives important results. In the following, we will first discuss the magnetic anisotropy of $La_{2-x}Sr_xCoO_4$ in terms of a one-electron picture. We will show that each spin state has a different magnetic anisotropy from which, by comparison to the experiment, the spin states of the Co ion can be concluded. In order to obtain also a quantitative description and to verify our simple argumentation we will present a full many-body crystal-field calculation afterwards.

Within a cubic crystal structure, the 3d states split into e_g orbitals and t_{2g} orbitals. The basis can be chosen as $\{3z^2 - r^2, x^2 - y^2\}$ and $\{xy, xz, yz\}$, respectively. A partially filled t_{2g} shell can produce a pseudo orbital moment of $\tilde{L} = 1$. Though the individual real wavefunctions d_{xy}, d_{yz} and d_{xz} of the basis themselves have a completely quenched orbital moment, their linear combinations are in general complex. Writing $d^x_{m_l}$, $d^y_{m_l}$ and $d^z_{m_l}$ as the orbital wave function with the orbital moment quantized along the axes x, y and z, respectively, one finds

$$d^x_{\pm 1} = \frac{1}{\sqrt{2}}(\pm d_{xy} + i d_{xz}), \tag{1}$$

$$d^y_{\pm 1} = \frac{1}{\sqrt{2}}(\pm d_{yz} + i d_{xy}), \tag{2}$$

$$d^z_{\pm 1} = \frac{1}{\sqrt{2}}(\pm d_{xz} + i d_{yz}). \tag{3}$$

In the limit of very large crystal field splittings $10Dq$ and with a partially filled t_{2g} shell, the moment is isotropic, despite the large orbital moment. In fact, the t_{2g} electrons are sometimes compared to p electrons [19].

Introducing a tetragonal distortion, the orbital moment becomes anisotropic. The tetragonal crystal field splits the cubic e_g states into non-degenerate a_{1g} and b_{1g} levels, while the t_{2g} states split into a non-degenerate b_{2g} state and a two-fold degenerate e_g level. As a basis for these states, the real orbital functions can also be used. The z-axis of the system is taken to be identical

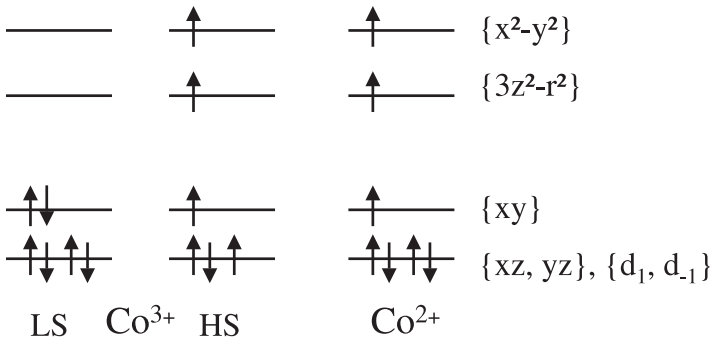

Figure 3. Splitting of the 3d levels in a tetragonal crystal field arising from an elongated oxygen octahedron. The two sketches on the left show the occupation for the LS and HS state of Co^{3+} in a one-electron picture. The right sketch refers to HS Co^{2+}. The real orbitals on the right can be used as a basis.

with the *c*-axis of the crystal. In the case of $La_{2-x}Sr_xCoO_4$, the oxygen octahedron is elongated in the *c*-direction. The order of levels and occupations for the ground states of the two cobalt ions is illustrated in figure 3.

The Co^{3+} LS is, except for a small Van Vleck susceptibility, nonmagnetic since it does not carry any moment. In the HS, Co^{3+} has spin and orbital moment. The orbital degeneracy is not completely quenched: the degenerate *xz* and *yz* are occupied by three electrons. These real orbitals can thus be recombined to form complex orbitals carrying orbital moment in the *z*-direction as described in equation (3). Note that the linear combinations in equations (1) and (2) cannot be formed because the *xy*-orbital is not degenerate with the *xz*- and *yz*-orbitals. Therefore the orbital moment is larger in the *z*-direction making this the easy axis. This anisotropy should be reflected in the susceptibility with $\chi_c > \chi_{ab}$, which obviously contradicts the anisotropy found in the measurements. A Co^{3+} HS system shows the wrong magnetic anisotropy.

Next, we discuss the IS state of Co^{3+}. Due to the elongation of the oxygen octahedra, the e_g electron occupies the $3z^2 - r^2$ orbital. This also affects the splitting of the t_{2g} states. The *xz*- and *yz*-orbitals remain degenerate but are not degenerate with the *xy*-orbital. This arises from the different charge distributions in relation to the $3z^2 - r^2$ orbital. We have five electrons to fill in the t_{2g} states, which can also be treated as one hole in the t_{2g} states. This hole is attracted to the e_g electron in the $3z^2 - r^2$ orbital. Figure 4 shows the charge distribution of this hole and the $3z^2 - r^2$ orbital. In the left sketch, both the electron in the $3z^2 - r^2$ orbital and a hole in the *xy*-orbital are drawn. The sketch in the center shows the $3z^2 - r^2$ orbital and the hole in a linear combination of the degenerate *xz*- and *yz*-orbitals. Regarding the distances between the electron and the hole, one can conclude that the state with the hole in the *xz*- and *yz*-orbitals is lower in energy. As the order of levels is reversed when we are speaking about holes instead of electrons, this means that the *xy*-orbital is lowered in energy. Thus, the order and occupation of levels is the one shown in figure 4. The magnetic anisotropy is the same as in the case of Co^{3+} HS which we treated in the last paragraph. With three electrons in the degenerate level of the *xz*- and *yz*-orbitals, we can also make use of equation (3) to show that the direction of anisotropy does not fit the measurements for $La_{2-x}Sr_xCoO_4$.

Neither the HS nor the IS state of Co^{3+} show the correct magnetic anisotropy. But before we draw further conclusions, Co^{2+} should be discussed. Although Co^{2+} has also been found in

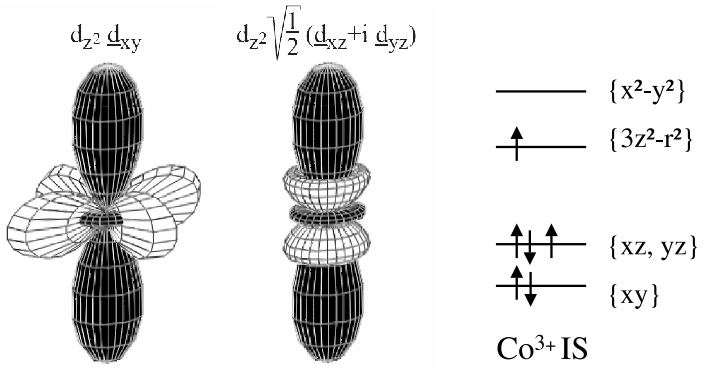

Figure 4. The picture on the left shows the charge distribution for an electron in the $3z^2 - r^2$ orbital (black) and a hole in the *xy*-orbital (white). The charge distribution in the center refers to an electron in the $3z^2 + r^2$ orbital and a hole in a linear combination of the *xz*- and *yz*-orbitals. The splitting and the occupation of the 3d levels for Co^{3+} in the IS state is shown on the right.

the LS state in some intramolecular compounds [20], for bulk crystals it can be safely assumed that Co^{2+} is in the HS state [22].

Regarding the ground state produced by the crystal field in figure 3, where the lowest level is filled, no linear combinations like in equation (3) can be formed. The orbital moment would be completely quenched and the magnetic moment would be determined by an isotropic spin. If, however, spin–orbit coupling is of the same magnitude as the splitting of the t_{2g} orbitals, it will mix these states. Mixing in a state with orbital moment in the *z*-direction would require placing a hole in the $d^z_{\pm 1}$ orbital (see equation (3)). This would cost an energy equal to the splitting within the t_{2g} orbitals. It is more favorable to mix in a state with orbital moment in the *x*- (or *y*-) direction by placing a hole in the $d^x_{\pm 1}$ (or the $d^y_{\pm 1}$) orbital (see equation (1)). This costs only half of the crystal-field splitting within the t_{2g} orbitals. An orbital moment in the *x*- (or *y*-) direction costs less energy than in the *z*-direction. So, the *xy*-plane will be the easy plane for Co^{2+} in this elongated tetragonal structure [24]. The spin moment will also be found in the *xy*-plane. Comparing these findings to the measurement, we see that Co^{2+} shows the correct direction of magnetic anisotropy. Now a conclusion about the spin state of Co^{3+} can be drawn. For $x \geqslant 0.5$, at least half of the cobalt ions in the crystal are Co^{3+}. Taking into account that Co^{2+} has a smaller spin moment than HS Co^{3+}, the latter would dominate the anisotropy. The opposite is, however, the case in the data. Thus, for this doping range, the spin state of Co^{3+} is identified with the LS state and the magnetization must be assigned to Co^{2+}, which shows the correct anisotropy. For $x = 0.4$, we still have 40% Co^{3+} and, because of the pronounced anisotropy, we can follow the same argumentation here. Regarding $x = 0.3$ in figure 2, the anisotropy is found to be rather small compared to the other compounds.

It should be stressed that the direction of anisotropy in layered perovskites depends on the direction in which the oxygen octahedron is distorted. In some systems like K_2CoF_4 the octahedra are compressed in the *c*-direction, resulting in an easy-axis anisotropy [23]; Co^{2+} in almost cubic symmetry also tends to have an easy-axis anisotropy like in CoO. However, in our case of $La_{2-x}Sr_xCoO_4$, the oxygen octahedron surrounding the cobalt ion is elongated by the inherent tetragonal structure. This situation is comparable to the change of anisotropy in CoO films on different substrates [22].

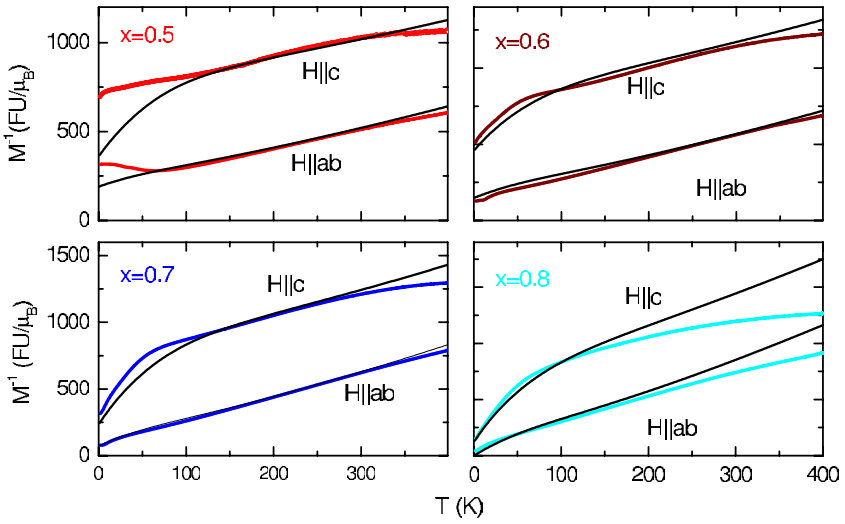

Figure 5. Measured magnetization (colored lines) compared with the calculation for Co^{2+} (black lines), plotted inverse. A mean-field magnetic exchange was added to the calculation. Note that the magnetization of the ion was weighted with the content of Co^{2+} $(1-x)$.

For a quantitative analysis of the data and a confirmation of the results found in the qualitative discussion of the anisotropy, a full-multiplet calculation was carried out within the crystal field approximation [24]. A Hamiltonian for the 3d shell of the Co^{2+} ion was set up, including crystal field, spin–orbit coupling and magnetic field. The Slater integrals F_0, F_2 and F_4 characterizing the Coulomb interaction and the spin–orbit coupling constant were taken from a Hartree–Fock approximation [25]. Any excitations from the oxygen 2p levels and mixing with higher states were neglected, as these effects are not significant when considering thermal energies. The parameters for the crystal field were treated semi-empirically. Regarding the tetragonal distortion as a perturbation of the cubic symmetry, the effect of the hybridization of the Co 3d shell with the surrounding oxygen 2p shells only increases the splitting of the cubic t_{2g} and e_g states. Hybridization can thus be included in the crystal field parameters and need not be treated separately. The Hamiltonian was diagonalized and eigenstates and eigenvalues were used to obtain the temperature dependence of the magnetization. Magnetic exchange was included in the calculation on a mean-field level. The results can be seen in figure 5, where the inverse magnetization is plotted.

The crystal-field parameters were chosen as follows: the $10Dq$ splitting and the splitting within the e_g levels were fixed at 1.5 and 0.2 eV, respectively. These two values are of minor importance for the calculation, because the anisotropy of the magnetization arises from the t_{2g} electrons, as described in the discussion above. The splitting of the t_{2g} states showed up to be crucial for the form and the anisotropy of the calculated curves. The values of the splitting within the t_{2g} states were chosen as 80, 60, 68 and 50 meV for the compounds $x = 0.5$, 0.6, 0.7 and 0.8, respectively. These t_{2g} crystal field splittings for Co are in good agreement with previous measurements on strained CoO thin films [22]. They might appear to be surprisingly small compared to the values found for the titanates [26, 27] in the order of 200 meV. The difference between Co and Ti can be understood by considering the radial extent of the d wavefunction and the transition metal–oxygen (TM–O) distance. The Co d wavefunction is much smaller than the

Ti d wavefunction, reducing the covalency and thereby the size of the crystal-field splitting. At the same time, the average TM–O distances of $La_{2-x}Sr_xCoO_4$ and $LaTiO_3$ are almost equal (≈2.02 Å for Co–O [16] and ≈2.04 Å for Ti–O [28]). This is related to the occupation of the anti-bonding e_g orbitals in a HS Co^{2+} compound which pushes the O atoms further away.

It can be seen in figure 5 that the calculation gives a good description for $x = 0.6$ and $x = 0.7$. The magnetization of the half-doped sample $x = 0.5$ is reproduced well for higher temperatures. At temperatures below the freezing temperature, the calculation cannot describe the system because magnetic order is not included in the model. The $x = 0.8$ sample is fitted well for lower temperatures. Above $T \approx 350$ K, the magnetization in the measurement is enhanced by another effect and results in a deviation from the calculation. This effect can be seen in all curves in figure 2, but at significantly higher temperatures. This increase of magnetization could arise from the thermal population of the Co^{3+} HS or IS state. But surely further measurements at higher temperatures are needed to confirm this assumption. Nevertheless, the full-multiplet calculation of a pure Co^{2+} system already succeeds in describing the main features of the magnetization for $x \geqslant 0.5$. This confirms that Co^{3+} is a LS system in this doping range.

In summary, the magnetic susceptibility of $La_{2-x}Sr_xCoO_4$ has been analyzed for two different directions of the external magnetic field. A definite anisotropy of the magnetic moment is found experimentally with $\chi_{ab} > \chi_c$. This direction of anisotropy does not match with the behavior of HS or IS Co^{3+}, whereas Co^{2+} in the HS state shows the correct single-ion anisotropy. Thus, the spin state of Co^{3+} for $x \geqslant 0.4$ must be the LS state. This conclusion is also confirmed by a full-multiplet calculation.

Acknowledgment

We acknowledge financial support by the Deutsche Forschungsgemeinschaft through SFB 608.

References

[1] Jonker G H and Van Santen J H 1953 *Physica* **XIX** 120
[2] Raccah P M and Goodenough J B 1967 *Phys. Rev.* **155** 932
[3] Abbate M, Fuggle J C, Fujimori A, Tjeng L H, Chen C T, Potze R, Sawatzky G A, Eisaki H and Uchida S 1993 *Phys. Rev.* B **47** 16124
[4] Korotin M A, Ezhov S Y, Solovyev I V, Anisimov V I, Khomskii D I and Sawatzky G A 1996 *Phys. Rev.* B **54** 5309
[5] Zobel C, Kriener M, Bruns D, Baier J, Grüninger M, Lorenz T, Reutler P and Revcolevschi A 2002 *Phys. Rev.* B **66** 020402
[6] Noguchi S, Kawamata S, Okuda K, Nojiri H and Motokawa M 2002 *Phys. Rev.* B **66** 94404
[7] Maris G, Ren Y, Volotchaev V, Zobel C, Lorenz T and Palstra T T M 2003 *Phys. Rev.* B **67** 224423
[8] Ropka Z and Radwanski R J 2003 *Phys. Rev.* B **67** 172401
[9] Lengsdorf R, Ait-Tahar M, Saxena S S, Ellerby M, Khomskii D I, Micklitz H, Lorenz T and Abd-Elmeguid M M 2004 *Phys. Rev.* B **69** 140403
[10] Baier J, Jodlauk S, Kriener M, Reichl A, Zobel C, Kierspel H, Freimuth A and Lorenz T 2005 *Phys. Rev.* B **71** 014443
[11] Haverkort M W *et al* 2006 *Phys. Rev. Lett.* **97** 176405
[12] Moritomo Y, Higashi K, Matsuda K and Nakamura A 1997 *Phys. Rev.* B **55** R14725
[13] Itoh M, Mori M, Moritomo Y and Nakamura A 1999 *Physica* B **259–61** 997–8

[14] Wang J, Tao Y C, Zhang W and Xing D Y 2000 *J. Phys.: Condens. Matter* **12** 7425–32
[15] Zaliznyak I A, Hill J P, Tranquada J M, Erwin R and Moritomo Y 2000 *Phys. Rev. Lett.* **85** 4353
[16] Cwik M 2007 *PhD Thesis* University of Cologne
[17] Bruno P 1989 *Phys. Rev.* B **39** 865
[18] Goodenough J B 1968 *Phys. Rev.* **171** 466
[19] Kamimura H 1956 *J. Phys. Soc. Japan* **11** 1171
[20] Brooker S, de Geest D J, Kelly R J, Plieger P G, Moubaraki B, Murray K S and Jameson G B 2002 *J. Chem. Soc., Dalton Trans.* 2080–7
[21] Goodenough J B 1963 *Magnetism and the Chemical Bond* (New York: Wiley)
[22] Csiszar S I, Haverkort M W, Hu Z, Tanaka A, Hsieh H H, Lin H J, Chen C T, Hibma T and Tjeng L H 2005 *Phys. Rev. Lett.* **95** 187205
[23] Folen V J, Krebs J J and Rubinstein M 1968 *Solid State Commun.* **6** 865
[24] Ballhausen C J 1962 *Introduction to Ligand Field Theory* (New York: McGraw-Hill)
Sugano S, Tanabe Y and Kamimura H 1972 *Multiplets of Transition-Metal Ions in Crystals* (New York: Academic)
[25] Haverkort M W 2004 *PhD Thesis* University of Cologne
[26] Haverkort M W *et al* 2005 *Phys. Rev. Lett.* **94** 056401
[27] Rückamp R *et al* 2005 *New J. Phys.* **7** 144
[28] Cwik M *et al* 2003 *Phys. Rev.* B **68** 060401